ISSN 1070-3284, Russian Journal of Coordination Chemistry, 2024, Vol. 50, No. 6, pp. 415–426. © Pleiades Publishing, Ltd., 2024.

Versatile Electronic and Structural Properties of Ruthenium-Mediated 1,4-Diaza-1,3-butadiene Ligands: A Review

A. S. Roy*

Department of Chemistry, New Alipore College, New Alipore, Kolkata, 700053 India

**e-mail: amitsaharoychem@gmail.com*

Received November 6, 2023; revised January 4, 2024; accepted February 29, 2024

Abstract—Ruthenium α-diimine complexes are widely known for their unique low-lying excited states and potent light absorption capabilities in the visible and NIR regions. A few specially constructed Ru α-diimine complexes have also shown enormous potential in the biomedical field. Several Ru-diimine complexes are well known for their catalytic activity. In this context, the simplest α-diimine system is 1,4-diaza-1,3-butadiene, abbreviated as (DAB/DAD), which received the greatest attention from the research communities. DAB ligands are redox-active. DAB ligands typically function as effective electron donors by employing lone pairs of nitrogen atoms and the π-electrons of the C=N bonds while coordinating the metal ion. The structural, electronic, and photophysical properties of the metal-mediated (DAB) complexes largely depend on the substitution of the ligand backbone as well as metal precursors. A versatile 'redox noninnocent' 1,4-diaza-1,3-butadiene motif can stabilise different oxidation states of ruthenium metal depending on the reaction conditions and the presence of co-ligands. The comparative studies of the structural and electrical characteristics of diverse ruthenium-DAB compounds are intriguing, which opens up a new route for researchers to utilise them in a variety of application domains. It is challenging and fascinating to determine the precise electronic structure of redox noninnocent diimine complexes in the presence of a 'redox active' metal like ruthenium. In this concise review, we provided a brief overview of the structural and electrical features of various Ru DAB complexes that solely comprise (–N=CH–CH=N–) fragments in the skeleton.

Keywords: ruthenium, α-diimine, 1,4-diaza-1,3-butadiene, redox-active ligand

DOI: 10.1134/S1070328423601449

INTRODUCTION

Transition metal complexes containing α-diimine ligands have been one of the most studied topics in coordination chemistry for the last few decades. Numerous transition and main-group metal complexes of distinct types of α-diimine ligands, as shown in Scheme 1 (**1**–**6**), have been in the literature. Among them, 1,4-diaza-1,3-butadiene (–N=CH–CH=N–) frame, referred to as DAB or DAD ligands, is the simplest motif of the α-diimine family [1–7]. DAB is a superb, flexible chelating ligand that has easily tunable steric and electrical properties [8].

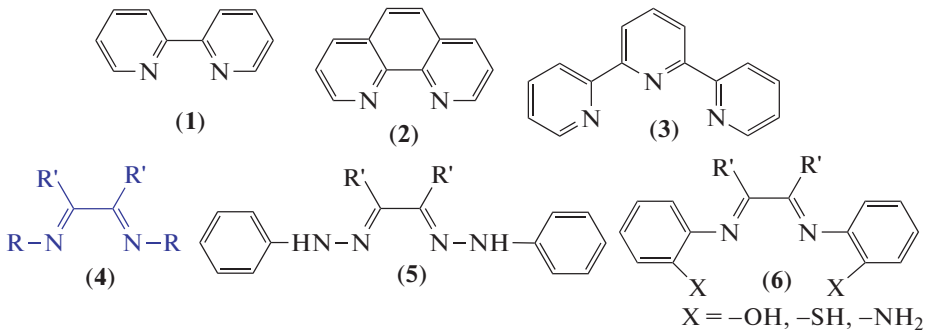

Scheme 1. Types of α-diimine fragments.

Catalysts and "molecular magnets" are successfully developed with these ligand fragments [9–11]. Interest in the chemistry of DAB complexes has increased substantially due to their potential uses in catalysis, specifically in hydrogen transfer [12], olefin epoxidation [13], ring-opening polymerization of cyclic esters [14–16], C–N cross-coupling reactions [17], hydroamination [18], hydrosilylation reactions [19], and other processes. The mechanism of the catalytic action on olefin polymerization by metal-medi-

ated DAB complexes, documented by Brookhart and co-workers, has significantly contributed to the understanding of diazadiene complex chemistry [20–22]. DAB also works as a key structural component in the synthesis of several heterocyclic compounds [23]. A wide range of transition [1–7, 24, 25], main-group [26, 27], and even rare earth metal complexes [28–30] of DAB ligands have been synthesised, and the potentiality of these complexes has been analysed based on experimental and theoretical results [31].

Most of the reviews so far published are focused on the main group and the early transition metal ion complexes with α-diimine ligands. In this review, we will refer to the 1,4-diaza-1,3-butadiene motif as DAB, and explore its potentiality exclusively with the ruthenium metal ion because the ruthenium-diimine complexes have several unique features and properties that draw special attention. Ruthenium-diimine complexes are well known for their distinctive photophysical characteristics, which include low-lying excited states and strong light absorption in the visible and near-IR region [32]. Boggio-Pasqua and co-workers extensively reported the theoretical comparisons between the photophysical characteristics of the ruthenium-diimine with the model complex $[Ru(bpy)_{3-x}(DAB)_x]^{2+}$ ($n = 1–3$) (bpy = bipyridine) [33]. Selected ruthenium-DAB chromophores also exhibit antibacterial and anticancer activity [34].

The electronic structure of the Ru-DAB complex depends on the features of the ruthenium metal precursor as well as the 1,4-diaza-1,3-butadiene (–N=CH–CH=N–) ligand backbone. The electronic properties are tuned by the cooperative effects of metal ions and ligands. The DAB has low-lying π* orbitals, a benchmark feature of the α-diimine system. DAB exhibits redox noninnocent behaviour that allows it to stabilise mixed-valent systems with redox active metals like ruthenium, which has dynamic redox states of (II), (III), (IV), and even the low-valent state (0). Assigning the correct electronic structure of such a coordination entity containing ruthenium metal and DAB ligands is challenging and interesting due to the composite nature of the redox states involved. These types of redox-active couples can participate in intra- or intermolecular electron transfer phenomena and exhibit valence-state (VT) tautomerization [35]. Comprehending the precise electrical configuration of these systems is imperative in order to create effective catalysts and understand their reactivity in diverse chemical reactions.

The general redox noninnocent behaviour of DAB systems has been extensively documented by the reviewers, including a special issue in the *European Journal of Inorganic Chemistry* [36], a recent Forum Issue in *Inorganic Chemistry* [37], a themed collection titled "Nitrogen Ligands" in *Dalton Transactions* [38], and some other reviews [39]. Nikolaevskaya and his associates reviewed the alkali and transition metal chemistry of the diazadiene-type ligand system having an extra coordinating group in the chromophore [3]. Mashima analysed the activity of early transition metal complexes in the presence of various diimine systems [24].

In most cases, DAB ligands are synthesized from the condensation of α-dicarbonyl or α-dialdehyde with different types of substituted aromatic amine and, in some cases, aliphatic amine (Scheme 1, (**4**)). A few other types of ligand systems are available where the additional –NH group is introduced in between R–N fragments, referred to as the osazone ligands system (Scheme 1, (5)), synthesised by swapping out the amine for a phenyl hydrazine or its derivative. The presence of a supporting coordinating group as a component of the phenyl ring generates another type of the α-diimine system, converting the bidentate diaza-1,3-butadiene motif to a tetradentate ligand (Scheme 1, (**6**)). For the sake of simplicity, we limit our discussion to the α-diimine ligand systems, which have no additional coordinating group. Additionally, the polypyridine diimine ligands in which the nitrogen atom is a part of an aromatic system and diimine derived from benzoquinones were not included in this analysis. We attempt to investigate the chemistry of various types of ligand systems generated by changing the substitution of R and R' in (Scheme 1, (**4**)) coupled with a ruthenium metal centre.

The specific structure and redox activity of the Ru-DAB chromophore have not yet been thoroughly scrutinized. Here, we address the comparative electrical and structural properties of the diverse Ru-diazabutadiene systems. The electronic structure and redox characteristics of the diimine coordinated to the ruthenium metal ion are the most exciting systems that we would like to emphasise in this brief discussion.

DIAZABUTADIENE LIGAND SYSTEMS

Diazadiene ligand systems have attracted a lot of interest in the last 40–60 years. Among the various α-diimine systems, the DAB ligand can be synthesised easily in high yield with minimal time and economical starting materials. Most of the time, dialdehyde or diketone are condensed with various aromatic or aliphatic amines to create DAB ligand systems (Scheme 2) [40]. DAB ligands have diverse bonding patterns and better π-acceptor capacity compared to rigid polypyridine rings like bipyridine [1, 41].

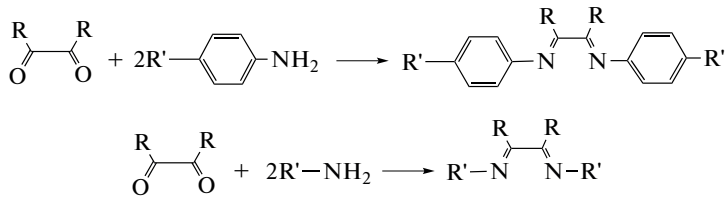

Scheme 2. General steps involved in preparing the DAB ligand system.

A coordinated diimine fragment (–N=CH–CH=N–) (Scheme 1, (4)) normally forms a stable five-member ring when coupled with the metal ion. The presence of conjugation (–N=CH–CH=N–) in the diazabutadiene allows π-electron density to operate throughout the system. Lone pairs on nitrogen atoms and the π-electrons of the C=N bonds make α-diimine fragments (4) efficient electron donors, allowing coordination with the metal ions using two, four, or (in uncommon circumstances) eight electron donors. Additionally, the two substituents on the (–N=CH–CH=N–) motif are able to adjust the ligand's steric and electronic characteristics. To tune these properties, various DAB ligands are synthesized by changing the N-substituted alkyl or aryl groups of the ligand system (4) (Scheme 3).

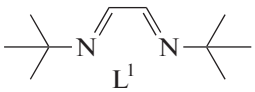

L^1

1,4-Di-*tert*-butyl-1,3-diazabutadiene

L^2

1,4-Dicyclohexyl-1,3-diazabutadiene

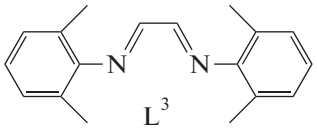

L^3

1,4-Bis(2,6-dimethylphenyl)-1,3-diazabutadiene

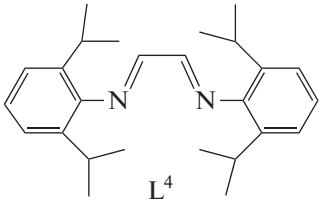

L^4

1,4-Bis(2,6-diisopropyl)-1,3-diazabutadiene

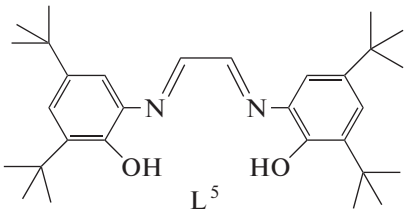

L^5

1,4-Bis(2-hydroxy-3,5-di-*tert*-butylphenyl)-1,3-diazabutadiene

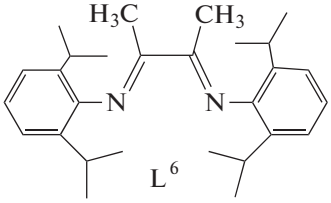

L^6

1,4-Bis(2,6-diisopropyl)-1,3-diaza-2,3-dimethylbutadiene

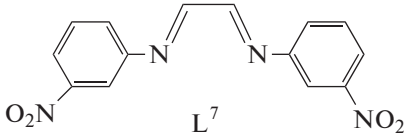

L^7

1,4-Di(3-nitrophenyl)-1,4-diazabutadiene

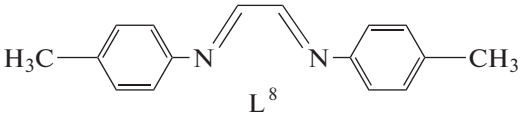

L^8

1,4-Di(4-methylphenyl)-1,4-diazabutadiene

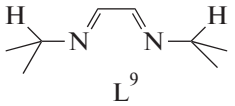

L^9

N,*N*'-Diisopropyl-1,4-diaza-1,3-butadiene

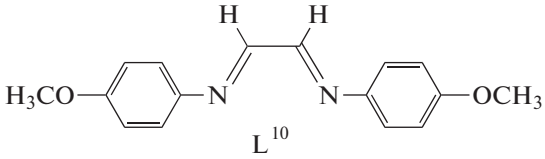

L^{10}

1,2-Bis-(*p*-methoxyphenylimino)ethane

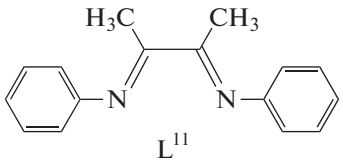

L^{11}

3-(Phenylimino)butan-2-ylidene benzenamine

Scheme 3. Different types of the diazabutadiene ligands.

DAB ligands have substantial π-back bonding capacity [35, 42], which effectively stabilises low-valent transition metal complexes such as $[Fe(DAB)_2]$ and $[Ni(DAB)_2]$ [43–45]. DAB ligands can show flexible behaviour during coordination with metal ions. It can act as monodentate, bidentate, or bridging ligands while coordinating metal ions [3, 8, 40]. DAB ligands in the *cis*-conformation behave as bidentate ligands, whereas, on rare occasions, in the *trans*-conformation, they can act as bridging ligands [4].

ELECTRONIC AND STRUCTURAL ASPECT OF THE DIIMINE MOTIF

Scheme 4 depicts the dynamic valence state of the DAB ligand as well as the probable binding mechanism of the ligand. Coordination chemists are extremely interested in investigating the varied valence states and the most likely binding modes of DAB ligands.

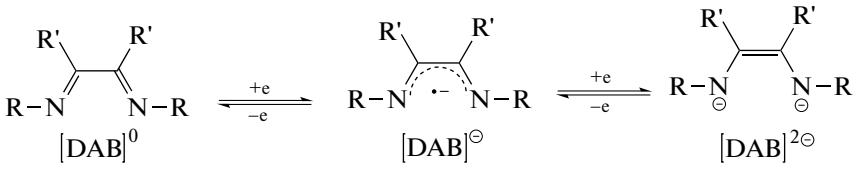

Scheme 4. Different electronic states of the DAB fragment.

The position and character of the substituents on the –N=HC–CH=N– backbone substantially influence the DAB ligand's redox activity. The diimine fragments readily accept an electron in their low-lying, lowest unoccupied molecular orbital (LUMO), thereby undergoing a one-electron reduction to form a diimine anion radical. Conjugated α-diimine fragments can exist in three different redox states: neutral diimine $(DAB)^0$ [46–48], monoanionic radical $(DAB)^{\bullet -}$ [49–58] and di-anionic diimide $(DAB)^{2-}$ [59–61]. The states are well defined with respect to precise bond parameters, spectral properties, redox potentials, and DFT calculations obtained from the analysis of several metal-coordinated diimine complexes reported in the literature.

Wieghardt [44, 52, 55] and the other groups have studied and reported the redox noninnocence of α-diimine ligands thoroughly while coordinating with the various transition metal ions. Identifying the particular electronic structure of complexes is challenging due to the possibility of numerous valence states. Both experimental techniques and theoretical calculations have been employed to elucidate the exact electronic structures of various homo- and heteroleptic complexes having redox noninnocent systems. Cui et al. investigated the bonding interaction with the dianionic and diamido states of DAB ligands thoroughly while coordinating *s*-, *p*-, and *f*-block metals [62]. Yang et al. in 2021 examined the structure and bonding of the main group metals with α-diimine ligands [63]. Very recently, DAB (in the reduced forms) complexes of earlier transition metals and *f*-block metals have been reviewed by Mashima [24].

As stated earlier, the diimine chromophore in the DAB ligand is electronically more flexible compared to bipyridine to readily accept excess electron density from the low-oxidation-state metal ion in its lowest unoccupied molecular orbital (LUMO). Diimine's C–C bonding LUMO can steal an electron from the electron-rich metal ion and generate a monoanionic radical ligand $(DAB)^{\bullet -}$ those results in a significant difference in C–C and C–N bond distances compared to the neutral diimine state.

Neutral DAB ligands usually have a C=N double bond (ca. 1.29 Å) and a C–C single bond length (ca. 1.50 Å), whereas in one electron reduce state $(DAB^{\bullet -})$, there are elongated C–N distances (1.32 Å) and shortened C–C distances (1.40 Å), resulting in averaged bond lengths due to delocalized electron density throughout the C_2N_2 backbone. In the dianionic state, the C–N distance is further elongated, and the C–C length is shortened [64].

In 1994, Raston et al. reported the single crystal X-ray structure of the series of paramagnetic bis(1,4-dialkyl-1,4 diazabutadiene) complexes, consisting of lithium (**7**), gallium, magnesium, and zinc. This structure unequivocally proves the neutral anionic radical state of the diimine system [65] (Scheme 5). When the X-ray crystallographic bond parameters of the above system are compared with the neutral diimine fragment, it has been noticed that the CN and CC distances are 1.24 and 1.49 Å, respectively, whereas in the diimine anion radical state, the average CN bond distance is 1.32 Å and the CC bond length is 1.40 Å. In fact, the structural behaviour of such a system is heavily influenced by the coordination mode of the metal ion. To determine the electronic properties of DAB complexes, different spectroscopic evidence must be analyzed to correlate with the X-ray crystallographic data. DFT simulations are also required for comprehensive analysis to determine the actual electronic structure of the complex.

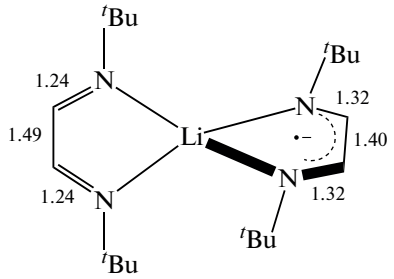

$[Li(^tBu_2DAB)_2]$

Scheme 5. Bond distances in Li(1,4-di-*tert*-butyl-1,4-diazabutadiene)$_2$.

In the literature, numerous main group as well as transition metal ion complexes with DAB ligands are reported, but specific structurally characterised ruthenium-coordinated 1,4-diaza-1,3-butadiene ligands are limited. The bond parameter and redox activity of several ruthenium-DAB systems are analysed in the next section in accordance with the sequential order accessible in the literature since 1980.

RUTHENIUM COMPLEXES OF 1,4-DIAZA-1,3-BUTADIENE LIGANDS

Chaudret and Poilblanc published the first study on diazadiene-ruthenium complexes in 1980 [66]. They reported four different N and C substituted diimine ligand systems (Scheme 3, L^1, L^9, L^{10}, and L^{11}), which are reacted with ruthenium metal precursors to ultimately form dinuclear ruthenium DAB complexes (Scheme 6).

$$DAB + [Ru(PPh_3)_2Cl_2] \longrightarrow [Ru_2(DAB)_2(PPh_3)_2Cl_3]X$$

$$X = Cl^- \text{ or } BPh_4^-$$

Scheme 6. A generic reaction strategy for synthesising $[Ru_2(DAB)_2(PPh_3)_2Cl_3]^+$.

On the basis of NMR and other spectroscopic evidence, the chloro-bridged dimer structure of ruthenium has been established. But no X-ray crystallographic data was available to validate the precise structures of these complexes. The following year (1981), the same group reported tris-DAB; (DAB = 1,2-bis-(*p*-methoxyphenylimino)ethane) (L^{10}) ligand complexes of Ru(0) with structural confirmation. This could be the first ruthenium-diazadiene complex to have single-crystal X-ray crystallographic structural data. Poilblanc et al. reported $[Ru(L^{10})_3]^0$ complex (**I**) (Scheme 7) obtained from the reaction between $[RuH_2(PPh_3)_4]$ or $[RuH(C_6H_4PPh_2)(PPh_3)_2(C_2H_4)]$ and (L^{10}) DAB ligand in toluene. The C=N bond lengths of the diimine fragment in the complex **I** range from 1.28 to 1.38 Å (mean 1.34(5) Å), whereas those of the imino CC bonds range from 1.33 to 1.45 Å (mean 1.37(5) Å). Bond length data suggested that in the complex **I**, L^{10} ligands may bind the metal ion in a neutral anionic state, but magnetic moment and chemical reactivity do not support this fact. Interestingly, the compound is diamagnetic below –10°C and turns paramagnetic at higher temperatures. In the presence of molecular oxygen and even the existence of too much diazadiene, complex **I** quickly oxidises to $[Ru(DAB)_3]^{2+}$ [67]. We found that the reactivity of the complexes was comprehensively reported by the same group of researchers later [68].

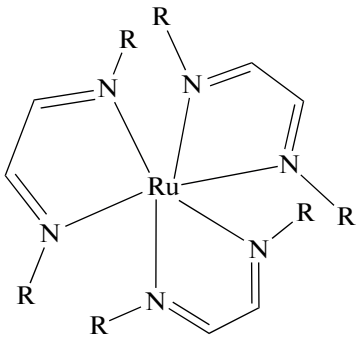

R = –C_6H_5OMe

Scheme 7. Schematic structure of **I**.

At almost the same time, the breakthrough in the chemistry of diazadienes was made by H. tom Dieck's group. H. tom Dieck et al. published the first octahedral ruthenium complex incorporating two *trans*-DAB ligands in 1981 [69]. The structure of *cis*-dichloro-bis(2,7-dimethyl-3,6-diazaoctadiene-3,5)ruthenium(II) (**II**) was synthesised from $RuCl_3 \cdot 3H_2O$ in the presence of Zn dust in THF solvent. The *cis*-configuration of the structure was confirmed from the ^1H NMR data. X-ray crystallography revealed that although the average C–C distance is shortened to 1.40 Å, the C=N bond lengths (1.29 Å) are only somewhat shorter than in a free DAB in the gas phase. These unambiguously indicate that ruthenium metal develops a back bonding interaction with the DAB ligand, implying the DAB ligand's monoanionic radical nature.

Later, they documented the synthesis of series $[Ru(DAB)_2C1_2]$ (**III**), where DAB = diazadiene, (RN=CR'–CR=NR) complexes, as well as their *trans-cis* isomerization, conformational, and spectroscopic properties. The symmetry and conformation of the compounds are explored using electronic spectra, ^1H NMR, and electrochemical data. The redox process between Ru(II) and Ru(III) is entirely reversible for both stereochemistrys, while the reduction is irreversible [70]. But at that time, all these complexes were not completely characterised by X-ray crystallography.

In 1987, H. tom Dieck et al. reported the synthesis, structure, and catalytic properties of another complex, [Ru(COD)(DAB)(H)Cl] (**IV**), where (DAB = 1,5-cyclooctadiene-1,4-diaza-1,3-diene). In this case, structure is also assumed based on a spectroscopy study [71]. They also reported that adding 2 equiv. of potassium in the THF complex $[Ru(DAB)_2C1_2]$ (**III**) (DAB = diazadiene, RN=CR'–CR=NR) was reduced to $[(DAB)_2Ru]$ (**V**). Complex **III** is further reduced by $(Mg–C_4H_6)$ in an argon environment, which results in a novel C–C coupling of butadiene to one of the diazadienes ligands. All these chemical processes were hypothesised with the aid of ^1H NMR and UV-vis data [72].

C.J. Elsevier and his co-worker reported the syntheses of a series of extremely air-sensitive mononuclear ruthenium-DAB complexes having the general formula [Ru(R-DAB)(CO)$_3$] (R-DAB: R = ^{i}Pr (**VI**), c-Hex (**VII**), ^{t}Bu (**VIII**), p-Tol (**IX**)) starting from $[Ru(CO)_5]$. Due to their extreme reactivity, these compounds could only be obtained in solution. Despite this, unambiguous characterization was achieved using IR, FD mass, ^1H NMR, and ^{13}C NMR spectroscopy. Yet, the author has further reported the synthesis and structural properties of the diruthenium complex $[Ru_2(^i$Pr-DAB)$(CO)_5]$ (**X**). Complex **X** has been generated thermally or photochemically from [Ru(^{i}Pr-DAB)(CO)$_3$] (**VI**). In **VI**, two reductively ^{i}Pr-DAB ligands are joined through the formation of a new C–C bond. As a result of this coupling, both N–C imine bonds have been reduced to aminato N–C bonds. Complex **VI** is unique for the generation of reversible carbon–carbon bonds and the simultaneous fission of two (^{i}Pr-DAB) ligands on a diruthenium fragment [73].

A bimetallic complex of the α-diimine system $[(CO)_5MnRu(Me)(CO)_2(^i$Pr-DAB)] (**XI**) (DAB = pyridine-2-carbaldehyde-*N*,*N*'-diisopropyl-1,4-diaza-1,3-butadiene) was reported by H.A. Nieuwenhuis et al. in 1995. Photochemical irradiation of the complex **XI** generates the formation of the radicals $[Mn(CO)_5^{\cdot}]$ and $[Ru(Me)(CO)_2(^i$Pr-DAB)$^{\cdot}]$. The existence of $[Ru(Me)(CO)_2(^i$Pr-DAB)] radicals has been confirmed by ESR spectroscopy [74].

In 1996, Maxim P. Aarnts synthesized a novel inorganometallic complex, $[Ru(SnPh_3)_2(CO)_2(^i$Pr-DAB)] (**XII**) (^{i}Pr-DAB = *N*,*N*'-diisopropyl-1,4-diaza-1,3-butadiene), and its stable radical-anion state $[Ru(SnPh_3)_2(CO)_2(^i$Pr-DAB$^{\cdot -})]$ (**XIII**) (Scheme 8). Complexes (**XII** and **XIII**) have a nearly linear Sn–Ru–Sn structural moiety. Interestingly, the central C–C bond (1.39(3) Å) of the ^{i}Pr-DAB ligand appears to be shorter in **XII** than in the closely related complex $[Ru(Cl)(SnPh_3)(CO)_2(^i$Pr-DAB)] (**XIV**) (1.435(6) Å). At the same time, the C–N bond distances are 1.34(2) and 1.34(3) Å, elongated with respect to **XIV** (1.279(6) and 1.303(6) Å). Complex **XII** is reversibly reduced at ($E_{1/2}$) –1.86 V vs. Fc/Fc$^+$. The chemical reversibility is documented by the peak current ratio (Ip$_a$/Ip$_c$). Electrochemical reversibility indicates that the reduction of **XII** is not accompanied by any major structural change, apparently producing the corresponding radical anion. The EPR signal, obtained in the THF solution, is centred at g = 1.9960. The EPR spectrum fully confirms the proposed composition of the $[Ru(SnPh_3)_2(CO)_2(^i$Pr-DAD$^{\cdot -})]$ radical species and also confirms the symmetry equivalence of the two Sn nuclei [75].

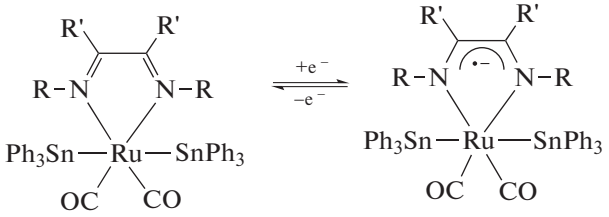

(XII) **(XIII)**

Scheme 8. Schematic structures of (**XII**) and (**XIII**.)

In 1997, Aarnts et al. reported the syntheses, structures, and spectroscopic properties of different bimetallic metal–metal bonded complexes of type $[Ru(SnPh_3)(Mn(CO)_5)(CO)_2(^i$PrDAB)] (**XV**), $[Ru(SnPh_3)(Co(CO)_4)(CO)_2(^i$PrDAB)] (**XVI**) and $[Ru(Re(CO)_5)_2(CO)_2(^i$PrDAB)] (**VII**) (^{i}PrDAB = *N*,*N*'-diisopropyl-1,4-diaza-1,3-butadiene). Complexes have a deformed octahedral geometry, according to X-ray crystallography data. The IR, Raman, NMR, and visible absorption spectra all exhibit charge-transfer bands in the visible region, with a significant $^4J(^{117,119}Sn,H)$ coupling constant for the DAB's imine protons, confirming the strong charge delocalization [76, 77].

Derk J. Stufkens reported in 1998 the synthesis and spectroscopic properties of *trans*,*cis* and *cis*,*cis* isomers of $[Ru(I)(Me)(CO)_2(^i$Pr-DAB)] (**XVIII**) [(^{i}Pr-DAB) = *N*,*N*'-diisopropyl 1,4-diazabutadiene] (Scheme 9). In these compound diimine, C–C bond length is 1.48(1), whereas the C–N bond lengths are 1.26(1) and 1.26(1) Å [78].

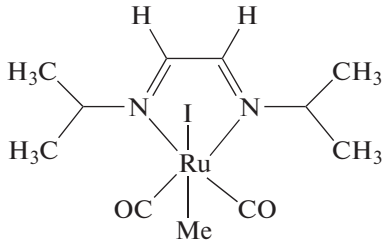

(**XVIII**)

Scheme 9. Schematic structure of (**XVIII**).

H.-W. Fruhauf et al. reported a stable ruthenium-DAB complex with carbonyl and iodide as coligands of type [(R-DAB)Ru(CO)$_2$I$_2$] (**XIX**) (R-DAB: *N*,*N*'-R$_2$-1,4-diaza-1,3-butadiene), which is analogous to [(^{i}Pr-DAB)Fe(CO)$_2$I$_2$] (**XX**). The C–N and C–C bond distances in these complexes, respectively, are 1.28 and 1.50 Å, whereas the ligand has practically equal bond distances of 1.258 and 1.457 Å, respectively, for the same bonds. This suggests that no metal-to-diimine-π-back bonding occurred [79].

J. van Slageren et al. extensively studied the ^{99}Ru NMR spectroscopy, UV-visible absorption spectra and theoretical perspective of the complexes of the type [Ru(X)(Y)(CO)$_2$(*i*-Pr-DAB)] (DAB: 1,4-diisopropyl-1,4-diaza-1,3-butadiene; X, Y = Ph_3Sn, Me_3Sn, Ph_3Pb, Ph_3Ge, Cl, Br, I, Me, Et, *i*-Pr, neo-Pe, [Mn(CO)$_5$], [RuCp(CO)$_2$)] [80, 81].

In 2009, Xue-Tai Chen and co-workers synthesized several Ru(II)–nitosyl complexes (**XXI**) (Scheme 10) in the presence of various diimine fragments, from [Ru(NO)Cl$_3$]. The Ru–N(imine) bonds in those complexes are in the range 2.052(4)–2.110(3) Å. Some of the Ru(II)–nitosyl complexes working as efficient catalyst precursors for the transfer hydrogenation of ketones and some of them exhibit catalytic activities in atom transfer radical polymerization of styrene [82].

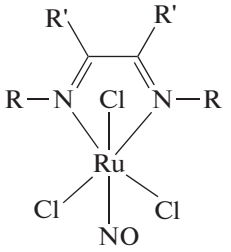

(**XXI**)

Scheme 10. Schematic structure of (**XXI**).

Wolfgang Kaim and co-authors published a several novel ruthenium coordinate diazabutadiene [Ru(R-DAB)(acac)$_2$] (**XXII**, **XXIII** and **XXIV**) in 2014 (R-DAB = 1,4-diorganyl-1,4-diazabuta-1,3-diene; *tert*-butyl,4-methoxyphenyl, 2,6-dimethylphenyl; acac = 2,4-pentanedionate) (Scheme 11). The average C–N bond length in these compounds is 1.317 Å, which is between 1.297 and 1.344 Å. The C–C bond lengths are 1.413 Å, which is intermediate between 1.382 and 1.425 Å. This bond length trend suggests an electronic structure of **XXII** is [Ru^{III}(R-DAB$^{\bullet-}$)(acac)$_2$], where the Ru(III) centre chelates with the monoanionic diazabutadiene radical system. All of these compounds are diamagnetic and EPR-silent. The analysis of bonding among **XXII**, **XXIII** and **XXIV** shows that substituting diimine fragments may influence the electrical features of the DAB ligand. According to experimental and theoretical studies, it has been concluded that metal-to-ligand π-back donation is more effective for the aryl-substituted DAB ligand compared to the *tert*-butyl-substituted DAB system. Crystallographic evidence, spectroscopic data analysis, the spin-orbit coupling constant and the average *g*-anisotropy value supported the coupling of the ligand-based radical system and the +3 oxidation state of the ruthenium metal [49].

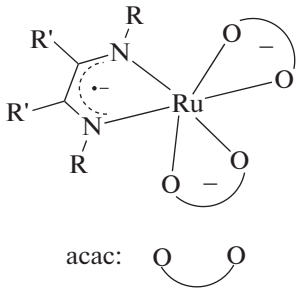

Scheme 11. Schematic structure of (**XXII**), (**XXIII**), and (**XXIV**) (R = 1,4-diorganyl-1,4-diazabuta-1,3-diene; -*tert*-butyl,4-methoxyphenyl, -2,6-dimethylphenyl; acac = 2,4-pentanedionate).

In 2014, our group [35] also reported the mononuclear ruthenium complex [Ru(DAB)(PPh_3)$_3$Cl$_2$] (**XXV**) (Scheme 12), starting from the precursor [Ru(PPh_3)$_3$Cl$_2$] and DAB ligand (DAB = 1,4-di(3-nitrophenyl)-1,4-diazabutadiene). The average Ru–P, Ru–Cl, and Ru–N distances are 2.4179(5), 2.4206(5), and 2.0519(14) Å as recorded crystallography data for the compound **XXV**.

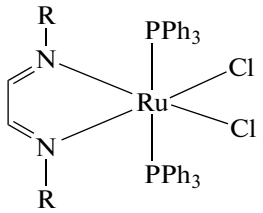

Scheme 12. Schematic structure of (**XXV**) (R = 1, 4-di(3-nitrophenyl)-1,4-diazabutadiene).

While complex **XXV** has lower energy absorption bands at 509 nm, the free DAB ligand (DAB = 1, 4-di(3-nitrophenyl)-1,4-diazabutadiene) absorbs strongly at 360 nm. Complex **XXV** exhibits reversible anodic peaks at 0.11 V and reversible cathodic peaks at −1.27 V. The redox activities of the complex **XXV** were

determined by cyclic voltammetry at 298 K in CH_2Cl_2. The anodic waves at +0.11 V are reversible, with reference to the Fc^+/Fc, ascribed to the Ru^{II}/Ru^{III} redox couple. This fact is backed by the EPR spectrum of the electrogenerated $[Ru(DAB)(PPh_3)_3Cl_2]^+$ cation. Similarly, due to the reduction of the diimine fragments, i.e., the formation of the [DAB/DAB$^{\bullet -}$] redox couple indicated by the reversible cathodic waves at 1.27 V. The EPR spectrum of electrogenerated $[Ru(DAB)(PPh_3)_3Cl_2]^-$ confirms the production of anion radicals.

$$[Ru^{III}(DAB)(PPh_3)_3Cl_2]^+ \underset{-1e}{\overset{+1e}{\rightleftharpoons}} [Ru^{II}(DAB)(PPh_3)_3Cl_2] \underset{-1e}{\overset{+1e}{\rightleftharpoons}} [Ru^{II}(DAB^{\bullet -})(PPh_3)_3Cl_2]^-.$$

The bond parameters, cyclic voltammetry analyses, EPR spectra, and DFT calculations have suggested that in the complex **XXV** neutral diimine fragments coordinate to a ruthenium(II) ion.

In 2018, Meng Guan Tay et al. reported the formation of dinuclear trichloro-bridged $[Ru_2Cl_3(P(p\text{-tolyl})_3)_2(OMe\text{-}DAB)_2]^+$ (**XXVI**) and mononuclear ruthenium $[RuCl_2(P(p\text{-tolyl})_3)_2(Me\text{-}DAB)]$ (**XXVII**) (Scheme 13) complexes. These complexes are synthesised from the reactions of chlorotris(*p*-tolylphosphine)ruthenium(II) with diazabutadiene ligands in THF. The two *trans*-mononuclear complexes were well characterized by X-ray crystallography as well as solid-state ^{31}P NMR. A temperature-dependent ^{31}P NMR study was carried out to monitor the formation of dinuclear and mononuclear complexes. Temperature-dependent ^{31}P and ^1H NMR experiments showed that the dinuclear complex was more favourable at low temperatures, whereas the mononuclear complex was more preferable at higher temperatures. When the bond lengths of free diimine and coordinated ligands were compared, the C=N-bond length increased from 1.28 to 1.31 Å after coordination with the Ru metal centre. In contrast, the length of the =CH–CH= bond decreased from 1.45 to 1.40 Å when compared to free diimines. In a Csp^2–Csp^2 conjugated system, the free diimine has a typical carbon-nitrogen double bond length, 1.28 Å, and a carbon-carbon single bond length, 1.45 Å. After coordination, the deformed diazadiene has longer –C=N– and shorter =CH–CH= bond lengths, indicating substantial π-back donation [83].

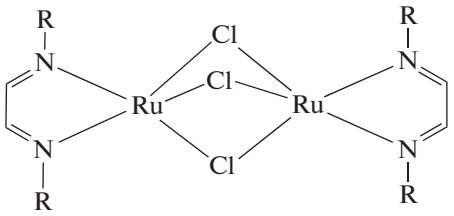

(**XXVI**)

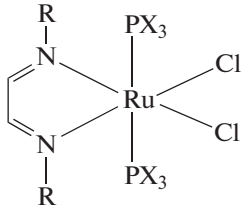

(**XXVII**)

Scheme 13. Schematic structure of (**XXVI**) and (**XXVII**) (R = 1,4-diazabutadiene; PX_3 = P(p-tolyl)$_3$).

S. Bhattacharya and co-workers recently developed a series of Ru-DAB complexes and explored their catalytic activity. Chloro-bridged di-ruthenium complexes (**XXVIII**) (Scheme 14) were generated from the reaction between $[Ru(PPh_3)_3Cl_2]$ and 1,4-diazabutadiene ligands (DAB = p-RC_6H_4N=C(H)–C(H)=NC_6H_4R-p; R = OCH_3, CH_3, H and Cl). These compounds' crystal structures were identified, and the DFT technique was used to optimise their molecular structure. These complexes have been shown to be effective catalyst precursors for the C–N coupling of primary amines under oxidative and deaminative conditions, yielding imines in good quantities [84].

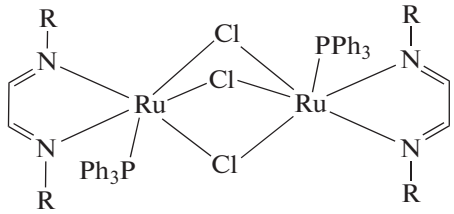

(**XXVIII**)

Scheme 14. Schematic structure of (**XXVIII**) (R = OCH_3, CH_3, H and Cl).

The same group of researchers further published the series of mononuclear complexes very recently, having a general skeleton *trans*-$Ru(DAB)_2Cl_2$ (**XXIX**). They have synthesized the *trans*-[$Ru(DAB)_2Cl_2$] complexes by refluxing *cis*-$Ru(DMSO)_4Cl_2$ with 1,4-diazabutadienes [DAB = *p*-$XC_6H_4N{=}C(H)(H)C{=}NC_6H_4X$-*p*; X = H, CH_3, OCH_3, and Cl] in acetone for 8 hours. On the other hand, the *cis*-analogous has been isolated by refluxing *ortho*-xylene for 10 hours. The *cis*-isomers are thermodynamically favourable and stable. The C–C and C–N bond lengths in the complexes are supported by the π-back-donation from the electron-rich, low-spin d^6 ruthenium centre to the DAB ligand motif. Cyclic voltammetry experiments on the complexes show an oxidative response and a reductive response within +0.50 to +0.93 V and –0.76 to –1.24 V vs. SCE, respectively. These complexes function as catalyst precursors for acceptor-less dehydrogenate coupling of primary alcohols to H_2 and esters [85].

SUMMARY

In this review, we have discussed numerous examples of N-substituted diazabutadiene ligand complexes and their coordination modes with distinct ruthenium metal centres. The findings, which were reported by numerous research groups over the last several decades, were examined using electronic structural features. Diazadiene is unequivocally a redox active ligand; it coordinates to the metal centre via neutral, mono-anionic, and dianionic states. It can stabilise the low- and high-oxidation states of ruthenium metal due to its diverse electronic state and bonding pattern. In most situations, ruthenium complexes are stabilised by the DAB ligand in the presence of other π-acid ligands such as CO, PPh_3, and so on. Bonding analysis of the complexes revealed that most of the cases involving ruthenium-mediated 1,4-diaza-1,3-butadiene motifs (–N=CH–CH=N–) have shorter NC and longer CC bond lengths. It is obvious due to the fact that diazadiene ligand can operate as both source and sink of the electron density, especially when bonded with the electron-rich Ru(II) d^6 metal ion. To determine the actual electronic structure of the system (Scheme 15), one must correlate all parameters, such as structural data, electrochemistry, EPR, and theoretical calculations [49].

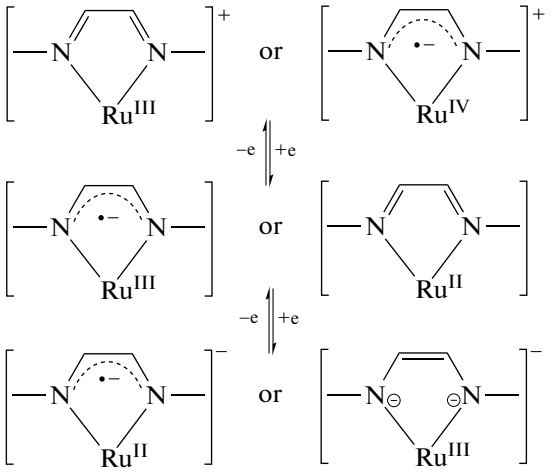

Scheme 15. Possible electronic states[$Ru^{n+}(DAB)_x^m$] system [49].

In this concise review, one can get brief information about the structure and binding mode of the 'redox active' ruthenium-diazadiene ligand systems.

ACKNOWLEDGMENTS

I am thankful to Dr. Jaydeep Sarangi, Principal, New Alipore College, Kolkata-700053, for his support and continuous encouragement to carry out research activities. A.S.R. acknowledges the New Alipore College research cell for sanctioning the projects (NAC/2022/177/12). I am thankful to Dr. Sachinath Bera, Assistant Professor of Chemistry, Shahid Matangini Hazra Govt. General Degree College for Women, for his valuable suggestions during the preparation of the manuscript.

FUNDING

This work was supported by ongoing institutional funding. No additional grants to carry out or direct this particular research were obtained.

CONFLICT OF INTEREST

As author of this work, I declare that I have no conflicts of interest.

REFERENCES

1. van Koten, G. and Vrieze, K., *Adv. Organomet. Chem.,* 1982, vol. 21, p. 151. https://doi.org/10.1016/S0065-3055(08)60380-9
2. Pashanova, K.I., Ershova, I.V., Yakushev, I.A., et al., *Polyhedron,* 2023, vol. 243, p. 116527. https://doi.org/10.1016/j.poly.2023.116527
3. Nikolaevskaya, E.N., Druzhkov, N.O., Syroeshkin, M.A., and Egorov, M.P., *Coord. Chem. Rev.,* 2020, vol. 417, p. 213. https://doi.org/10.1016/j.ccr.2020.213353

4. Voronina, J.K., Gavronova, A.S., Yambulatov, D.S., et al., *Russ. J. Coord. Chem.,* 2022, vol. 48, p. 916. https://doi.org/10.1134/S1070328422700154
5. Yambulatov, D.S., Nikolaevskii, S.A., Babeshkin, K.A., et al., *Russ. Chem. Bull.*, 2021, vol. 70, p. 2390. https://doi.org/10.1007/s11172-021-3358-1
6. Maier, T.M., Gawron, M., Coburger, P., et al., *Inorg. Chem.,* 2020, vol. 59, p. 16035. https://doi.org/10.1021/acs.inorgchem.0c02606
7. Barker, N.M., Li, Y.-X., McMillin, D.R., et al., *Inorg. Chem.,* 2019, vol. 58, p. 10716. https://doi.org/10.1021/acs.inorgchem.9b00669
8. Biancalana, L., Batchelor, L.K., Funaioli, T., et al., *Inog. Chem.,* 2018, vol. 57, p. 6669. https://doi.org/10.1021/acs.inorgchem.8b00882
9. Demir, S., Jeon, I.-R., Long, J.R., and Harris, T.D., *Coord. Chem. Rev.,* 2015, vols. 289–290, p. 149. https://doi.org/10.1016/j.ccr.2014.10.012
10. Trifonov, A.A., Shestakov, B., Long, J., et al., *Inorg. Chem.*, 2015, vol. 54, p. 7667. https://doi.org/10.1021/acs.inorgchem.5b01318
11. Klementyeva, S.V., Petrov, P.A., Starikova, A.A., and Konchenko, S.N., *Chemistry Select.,* 2018, vol. 3, p. 1262. https://doi.org/10.1002/slct.201703168
12. Saha, R., Mukherjee, A., and Bhattacharya, S., *Eur. J. Inorg. Chem.,* 2020, vol. 2020, p. 4539. https://doi.org/10.1002/ejic.202000859
13. Valente, A.A., Moreira, J., Lopes, A.D., et al., *New J. Chem.,* 2004, vol. 28, p. 308. https://doi.org/10.1039/b311114h
14. Mahrova, T.V., Fukin, G.K., Cherkasov, A.V., et al., *Inorg. Chem.,* 2009, vol. 48, p. 4258. https://doi.org/10.1021/ic802427f
15. Panda, T.K., Kaneko, H., Pal, K., et al., *Organometallics,* 2010, vol. 29, p. 2610. https://doi.org/10.1021/om1003144
16. Shestakov, B.G., Makhrova, T.V., Lyssenko, K.A., and Trifonov, A.A., *Russ. Chem. Bull.,* 2013, vol. 62, p. 412. https://doi.org/10.1007/s11172-013-0055-8
17. Mukherjee, A., Basu, S., and Bhattacharya, S., *Inorg. Chim. Acta.,* 2020, vol. 500, p. 119228. https://doi.org/10.1016/j.ica.2019.119228
18. Yakub, A.M., Moskalev, M.V., Bazyakina, N.L., et al., *Russ. Chem. Bull.*, 2016, vol. 65, p. 2887. https://doi.org/10.1007/s11172-016-1673-8
19. Anga, S., Naktode, K., Adimulam, H., and Panda, T.K., *Dalton Trans.*, 2014, vol. 43, p. 14876. https://doi.org/10.1039/C4DT02013H
20. Zhao, M. and Chen, C., *ACS Catal.*, 2017, vol. 7, p. 7490. https://doi.org/10.1021/acscatal.7b02564
21. Liu, Y., Yang, G., Li, C., et al., *Polym. Chem.*, 2024, vol. 15, p. 40. https://doi.org/10.1039/D3PY01011B
22. Ittel, S.D., Johnson, L.K., and Brookhart, M., *Chem. Rev.*, 2000, vol. 100, p. 1169. https://doi.org/10.1021/cr9804644
23. Heredia-Moya, J., Zurita, D.A., Cadena-Cruz, J.E., et al., *Molecules,* 2022, vol. 27, p. 6708. https://doi.org/10.3390/molecules27196708
24. Mashima, K., *Bull. Chem. Soc. Jpn.*, 2020, vol. 93, p. 799.
25. Yang, H., Zhao, Y., Bin, L., et al., *Dalton Trans.,* 2017, vol. 46, p. 7857. https://doi.org/10.1039/C7DT00455A
26. Wilson, H.H., Koellner, C.A., Hannan, Z.M., et al., *Inorg. Chem.,* 2018, vol. 57, p. 9622. https://doi.org/10.1021/acs.inorgchem.8b00045
27. Lieu, T. and Daugulis, O., *Organometallics,* 2022, vol. 41, p. 3249. https://doi.org/10.1021/acs.organomet.2c00264
28. Yan, H., Wu, B., Meng, Y.-.S., et al., *Inorg. Chem.,* 2021, vol. 60, p. 1315. https://doi.org/10.1021/acs.inorgchem.0c03534
29. Yan, H., Wei, J., and Zhang, W.-X., *Organometallics,* 2021, vol. 40, p. 3245. https://doi.org/10.1021/acs.organomet.1c00268
30. Duraisamy, R., Liebing, P., Harmgarth, N., et al., *ACS Omega*, 2020, vol. 5, p. 19061. https://doi.org/10.1021/acsomega.0c02414
31. de Zwart, F.J., Reus, B., Laporte, A.H.H., et al., *Inorg. Chem.*, 2021, vol. 60, p. 3274. https://doi.org/10.1021/acs.inorgchem.0c03685
32. Gabrielsson, A., Towrie, M., Záliš, S., and Vlček, A., Jr., *Inorg. Chem.,* 2008, vol. 47, p. 4236. https://doi.org/10.1021/ic702304k
33. Guillon, T. and Boggio-Pasqua, M., *Inorg. Chem.,* 2010, vol. 49, p. 8862. https://doi.org/10.1021/ic1009863
34. Zanda, E., Busto, N., Biancalana, L., et al., *Chem.-Biol. Interact.*, 2021, vol. 344, p. 109522. https://doi.org/10.1016/j.cbi.2021.109522
35. Patra, S.C., Roy, A.S., Manivannan, V., et al., *Dalton Trans.,* 2014, vol. 43, p. 13731. https://doi.org/10.1039/C4DT01241K
36. Hindson, K. and de Bruin, B., *Eur. J. Inorg. Chem.*, 2012, vol. 3, p. 340.
37. Chirik, P.J., *Inorg. Chem.,* 2011, vol. 50, p. 9737. https://doi.org/10.1021/ic201881k
38. Pombeiro, A.J.L., *Dalton Trans.,* 2019, vol. 48, p. 13904. https://doi.org/10.1039/C9DT90195G
39. Zhu, D., Thapa, I., Korobkov, I.S., et al., *Inorg. Chem.,* 2011, vol. 50, p. 9879. https://doi.org/10.1021/ic2002145
40. Raghavan, A. and Venugopal, A., *J. Coord. Chem.*, 2014, vol. 67, p. 2530. https://doi.org/10.1080/00958972.2014.931576
41. Sieger, M., Wanner, M., Kaim, W., et al., *Inorg. Chem.*, 2003, vol. 42, p. 3340. https://doi.org/10.1021/ic026078t

42. Balk, R.W., Stufkens, D.J., and Oskam, A., *Inorg. Chim. Acta,* 1978, vol. 28, p. 133.

43. tom Dieck, H. and Bruder, H., *Chem. Commun.,* 1977, p. 24. https://doi.org/10.1039/C39770000024

44. Muresan, N., Chlopek, K., Weyhermüller, T., et al., *Inorg. Chem.*, 2007, vol. 46, p. 5327. https://doi.org/10.1021/ic700407m

45. Lichtenberg, C., Adelhardt, M., Gianetti, T.L., et al., *ACS Catalysis*, 2015, vol. 5, p. 6230. https://doi.org/10.1021/acscatal.5b01416

46. Corn, I.R. and Sánchez, P.D.A., *Inorg. Chem.,* 2013, vol. 52, p. 5457. https://doi.org/10.1021/ic400348j

47. Kraft, S.J. and Williams, U.J., *Inorg. Chem.*, 2011, vol. 50, p. 9838. https://doi.org/10.1021/ic2002805

48. Hartl, F., Aarnts, M.P., Nieuwenhuis, H.A., and Slageren, J.V., *Coord. Chem. Rev.*, 2002, vol. 230, p. 107.

49. Grupp, A., Bubrin, M., Ehret, F., et al., *Eur. J. Inorg. Chem.* 2014, p. 110. https://doi.org/10.1002/ejic.201301206

50. Tsurugi, H., Saito, T., Tanahashi, H., et al., *J. Am. Chem. Soc.,* 2011, vol. 133, p. 18673. https://doi.org/10.1021/ja204665s

51. Khusniyarov, M.M., Weyhermüller, T., Bill, E., and Wieghardt, K., *J. Am. Chem. Soc.*, 2009, vol. 131, p. 1208. https://doi.org/10.1021/ja808149k

52. Ghosh, M., Sproules, S., Weyhermüller, T., and Wieghardt, K., *Inorg. Chem.*, 2008, vol. 47, p. 5963. https://doi.org/10.1021/ic800290s

53. Patra, S.C., Biswas, M.K., Maity, A.K., and Ghosh, P., *Inorg. Chem.*, 2011, vol. 50, p. 1331. https://doi.org/10.1021/ic101945d

54. Baker, R.J., Farley, R.D., Jones, C., et al., *Chem. Eur. J.*, 2005, vol. 11, p. 2972.

55. Ghosh, P., Bill, E., Weyhermüller, T., et al., *J. Am. Chem. Soc.*, 2003, vol. 125, p. 1293. https://doi.org/10.1021/ja021123h

56. Geoffrey, F., Cloke, N., Dalby, C.I., et al., *J. Chem. Soc. Chem. Commun.,* 1990, p. 1394. https://doi.org/10.1039/C39900001394

57. Kaim, W., Ernst, S., and Kasack, V., *J. Am. Chem. Soc.,* 1990, vol. 112, p. 173. https://doi.org/10.1021/ja00157a028

58. Kaim, W., *Coord. Chem. Rev.,* 1987, vol. 76, p. 187.

59. Gayathri, S., Viswanathamurthi, P., Bertani, R., and Sgarbossa, P., *ACS Omega,* 2022, vol. 7, p. 33107. https://doi.org/10.1021/acsomega.2c03200

60. Liu, Y., Yang, P., Yu, J., et al., *Organometallics*, 2008, vol. 27, p. 5830. https://doi.org/10.1021/om800554q

61. Greulich, S., Kaim, W., Stange, A.F., et al., *Inorg. Chem.,* 1996, vol. 35, p. 3998. https://doi.org/10.1021/ic9514814

62. Bai, Y., Chen, W., Li, J., and Cui, C., *Coord. Chem. Rev.*, 2019, vol. 383, p. 132.

63. Zhang, R., Wang, Y., Zhao, Y., et al., *Dalton Trans.,* 2021, vol. 50, p. 13634. https://doi.org/10.1039/D1DT02120F

64. Makhrova, T.V., Fukin, G.K., Cherkasov, A.V., and Trifonov, A.A., *Russ. Chem. Bull.,* 2008, vol. 57, p. 2285.

65. Gardiner, M.G., Hanson, G.R., Henderson, M.J., et al., *Inorg. Chem.,* 1994, vol. 33, p. 2456. https://doi.org/10.1021/ic00089a024

66. Chaudret, B. and Poilblanc, R., *J. Chem. Soc., Dalton Trans.,* 1980, p. 539. https://doi.org/10.1039/DT9800000539

67. Chaudret, B., Koster, H., and Poilblanc, R., *Chem. Commun.,* 1981, p. 266. https://doi.org/10.1039/C39810000266

68. Chaudret, B., Cayret, C., Koster, H., and Poilblanc, R., *Dalton Trans.*, 1983, p. 941. https://doi.org/10.1039/DT9830000941

69. Pank, V., Klaus, J., von Deuten, K., et al., *Transition Met. Chem.,* 1981, vol. 6, p. 185. https://doi.org/10.1007/BF00624342

70. Dieck, H.T., Kollvitz, W., and Kleinwaechter, I., *Inorg. Chem.,* 1984, vol. 23, p. 2685. https://doi.org/10.1021/ic00185a027

71. tom Dieck, H., Kleinwkzhter, I., and Haunt, E.T.K., *J. Organomet. Chem.*, 1987, vol. 321, p. 237. https://doi.org/10.1016/0022-328X(87)85043-X

72. Rosenberger, H. and tom Dieck, H., *Chem. Ber.*, 1990, vol. 123, p. 83.

73. Mul, W.P., Elsevier, C.J., Fruhauf, H.W., et al., *Inorg. Chem.*, 1990, vol. 29, p. 2336. https://doi.org/10.1021/ic00337a029

74. Nieuwenhuis, H.A., van Loon, A., Moraal, M.A., et al., *Organomet. Chem.,* 1995, vol. 492, p. 165. https://doi.org/10.1016/0022-328X(94)05300-Z

75. Aarnts, M.P., Wilms, M.P., Peelen, K., et al., *Inorg. Chem.,* 1996, vol. 35, p. 5468. https://doi.org/10.1021/ic960042h

76. Aarnts, M.P., Oskam, A., Stufkens, D.J., et al., *J. Organomet Chem.*, 1997, vol. 531, p. 191. https://doi.org/10.1016/S0022-328X(96)06726-5

77. Aarnts, M.P., Hartl, F., Peelen, K., et al., *Organometallics*, 1997, vol. 16, p. 4686. https://doi.org/10.1021/om9702800

78. Kleverlaan, C.J., Stufkens, D.J., Fraanje, J., and Goubitz, K., *Eur. J. Inorg. Chem.*, 1998, p. 1243.
79. Breuer, J., Fruehauf, H.-W., Smeets, W.J.J, and Spek, A.L., *Inorganic Chim. Acta,* 1999, vol. 291, p. 438.
80. Gaemers, S., Slageren, J., van O'Connor, C.M., et al., *Organometallics*, 1999, vol. 18, p. 5238. https://doi.org/10.1021/om990477n
81. Turki, M., Daniel, C., Zális, S., et al., *J. Am. Chem. Soc.,* 2001, vol. 123, p. 11431. https://doi.org/10.1021/ja010782b
82. Xu, H.-J., Lu, X.-Y., Chen, Y., et al., *Organometallics,* 2009, vol. 28, p. 6687. https://doi.org/10.1021/om9006714
83. Tay, M.G., Chia, Y.Y., and Kuan, S.H.C., *Transition Met. Chem.,* 2019, vol. 44, p. 293. https://doi.org/10.1007/s11243-018-00293-0
84. Saha, R., Mukherjee, A., and Bhattacharya, S., *New J. Chem.*, 2023, vol. 47, p. 12709. https://doi.org/10.1039/D3NJ01030A
85. Mukherjee, A., Datta, S., Richmond, M.G., and Bhattacharya, S., *RSC Adv.*, 2023, vol. 13, p. 25660. https://doi.org/10.1039/D3RA04750D